eLIFE
elifesciences.org

Figures and figure supplements

Flagellar synchronization through direct hydrodynamic interactions

Douglas R Brumley, et al.

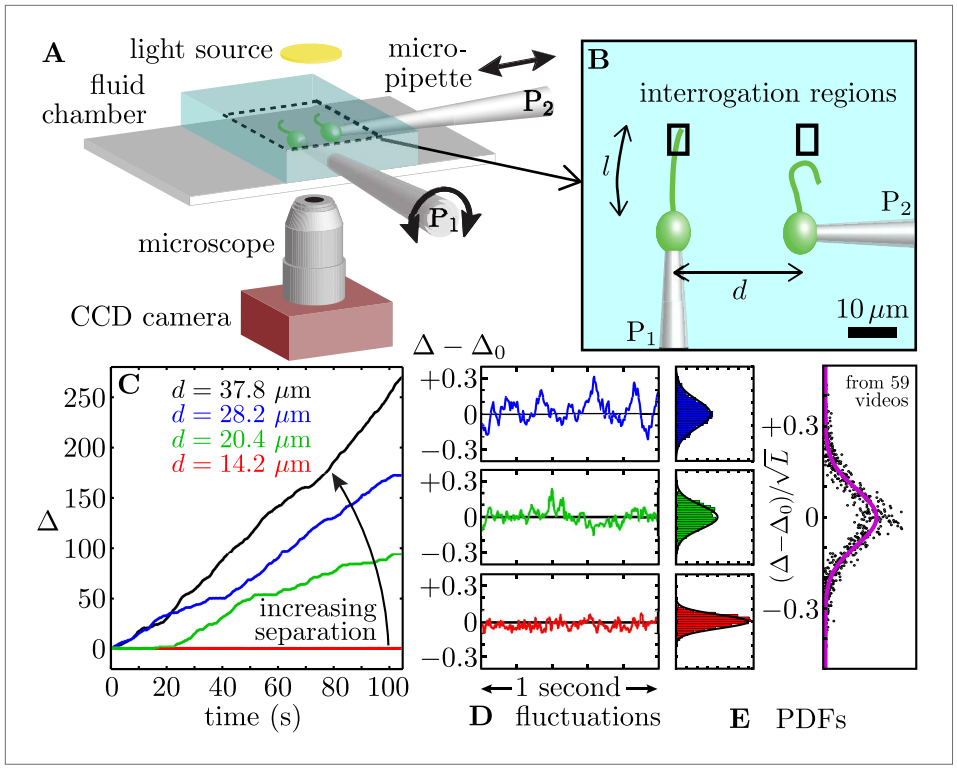

Figure 1. Synchronized pairs of beating flagella. (**A**) Experimental apparatus and (**B**) cell configuration. (**C**) Extracted phase difference $\Delta = (\varphi_1 - \varphi_2)/2\pi$ at four different interflagellar spacings, as indicated. These separations correspond to scaled spacing $L = d/l$ of 0.85, 1.22, 1.69, and 2.27. (**D**) fluctuations during phase-locked periods around the average phase lag, Δ_0, and (**E**) the fluctuations' probability distribution functions (PDFs), each cast in terms of the rescaled separation-specific variable $(\Delta - \Delta_0)/\sqrt{L}$. Solid lines represent Gaussian fits. Further details of the phase extraction procedure can be found in ***Figure 1—figure supplement 1***. Samples of the four processed videos corresponding to the cells in ***Figure 1C*** are shown in ***Video 1***.

DOI: 10.7554/eLife.02750.003

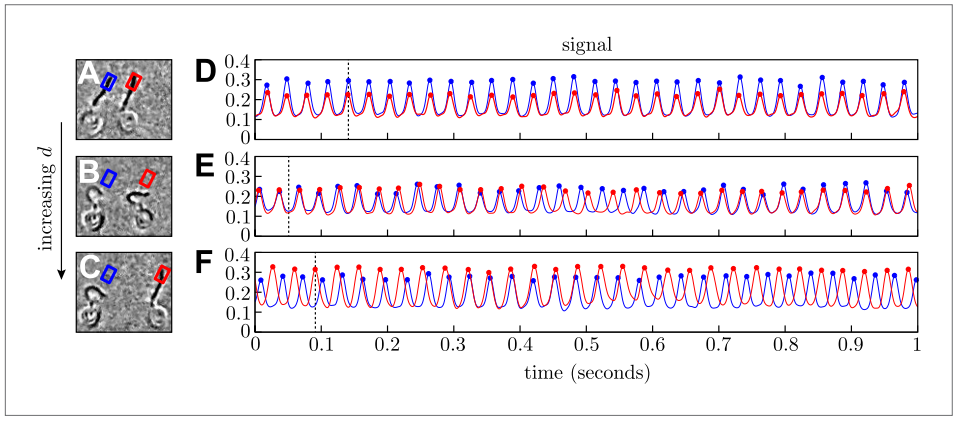

Figure 1—figure supplement 1. Phase extraction.

DOI: 10.7554/eLife.02750.004

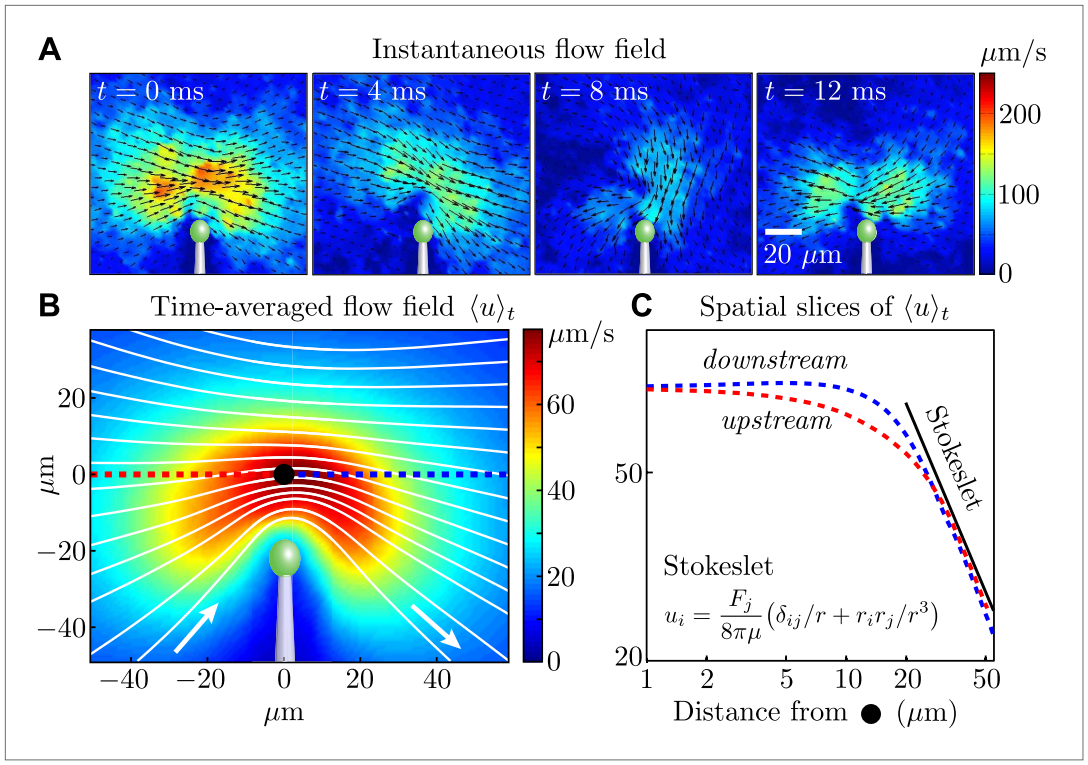

Figure 2. Measured flagellar flow field. (**A**) Time-dependent flow field for an individual cell measured using particle image velocimetry. Results are shown for the first half of the beating cycle. (**B**) Time-averaged flow field $\langle u \rangle_t = (1/\tau)\int_0^\tau |\boldsymbol{u}(\boldsymbol{x},t)|\,dt$ (averaged across 4 cells with $\tau \sim 1000$ beats for each). The velocity magnitude (colour) and streamlines (white) are shown. (**C**) Velocity magnitude *upstream* (red) and *downstream* (blue) of the origin (black dot in **B**).

DOI: 10.7554/eLife.02750.005

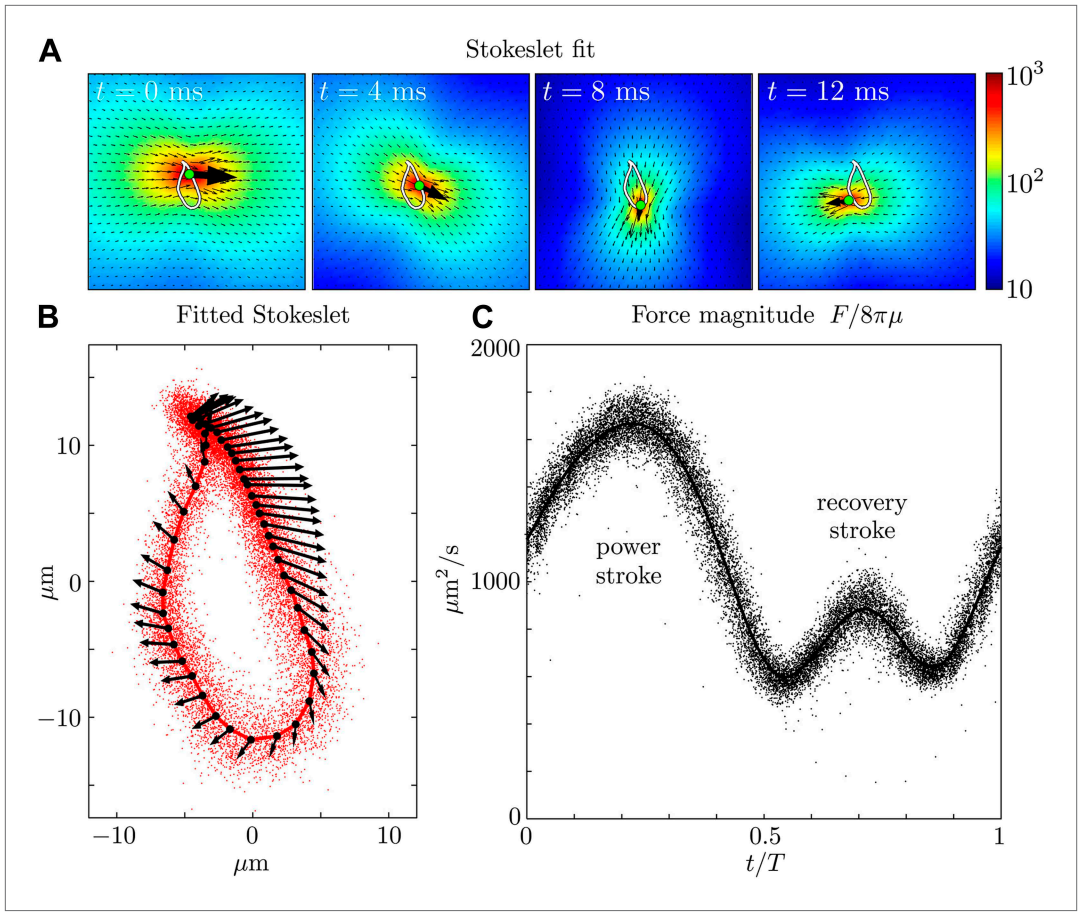

Figure 3. Force amplitude of flagellum. (**A**) Fitted instantaneous velocity field at various stages during the first half of one representative flagellar beat. (**B**) The fitted Stokeslet is shown at evenly-spaced times throughout the average flagellar beat cycle. The red dots indicate the Stokeslet position extracted from every frame. (**C**) Amplitude of the fitted point force as a function of time throughout the flagellar beat period *T*.

DOI: 10.7554/eLife.02750.006

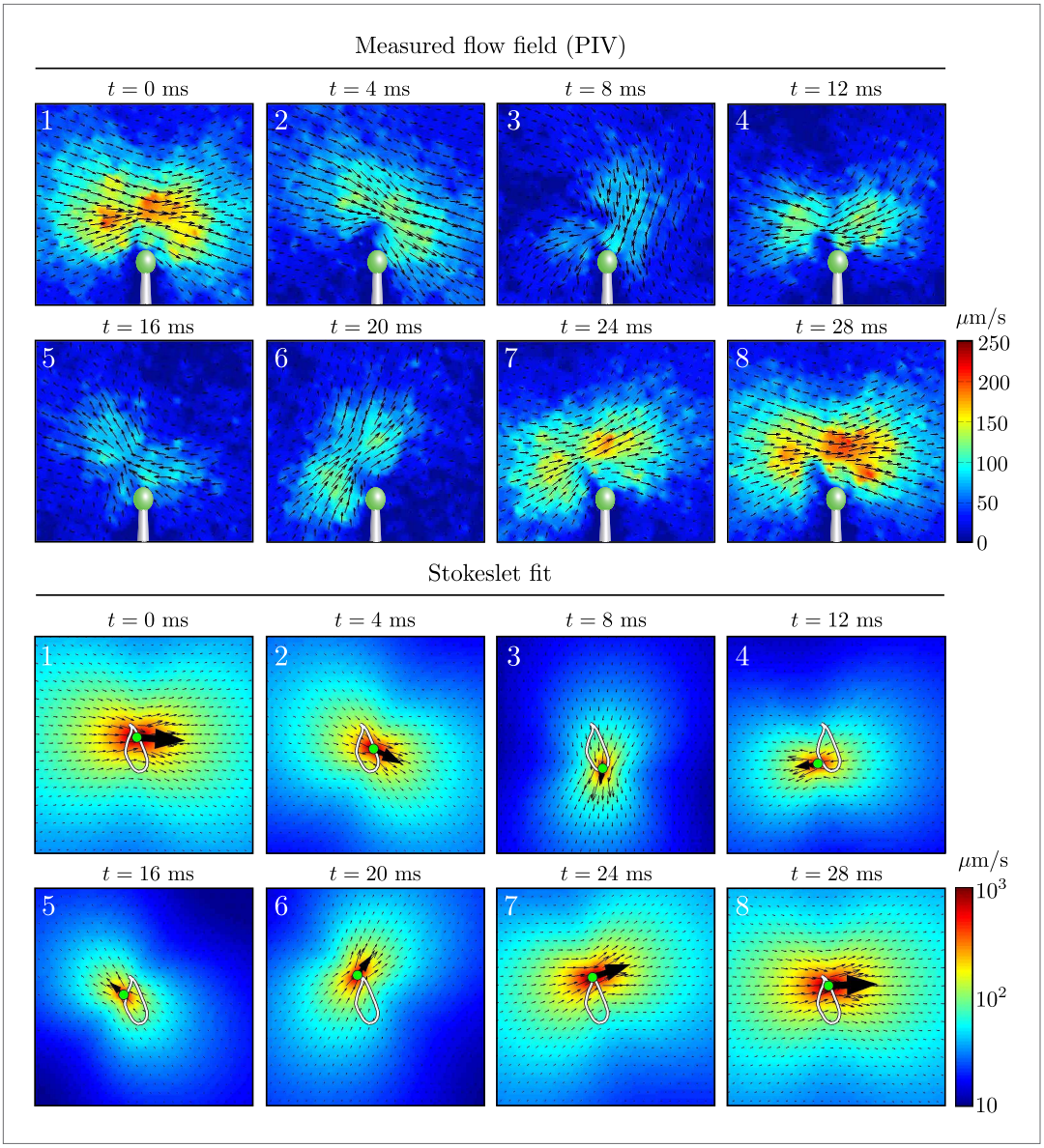

Figure 3—figure supplement 1. Time-dependent flow fields.

DOI: 10.7554/eLife.02750.007

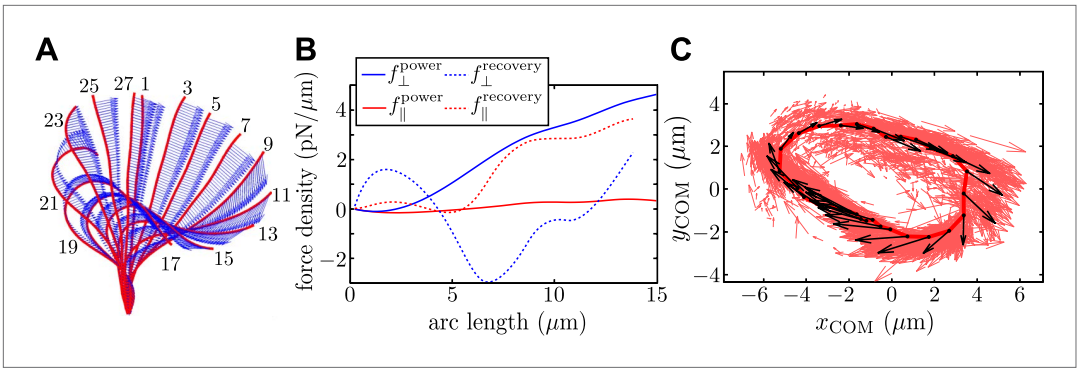

Figure 4. Resistive force theory analysis. (**A**) Instantaneous velocity distribution along the flagellum during one complete beat cycle (indexed by frame number, imaged at 1000 fps). (**B**) Components of integrated force density produced by a flagellum executing characteristic power and recovery strokes, as a function of arclength along the flagellum measured from the basal to the distal end. (**C**) Integrated vector forces $\boldsymbol{F}(t)$ shown localised at centre-of-mass coordinates $\boldsymbol{x}(t)$ (red: per frame, black: averaged over O(10^3) frames), evolve cyclically around an average trajectory. The average value is $|\mathbf{F}|/8\pi\mu \sim 1910\ \mu m^2/s$.

DOI: 10.7554/eLife.02750.008

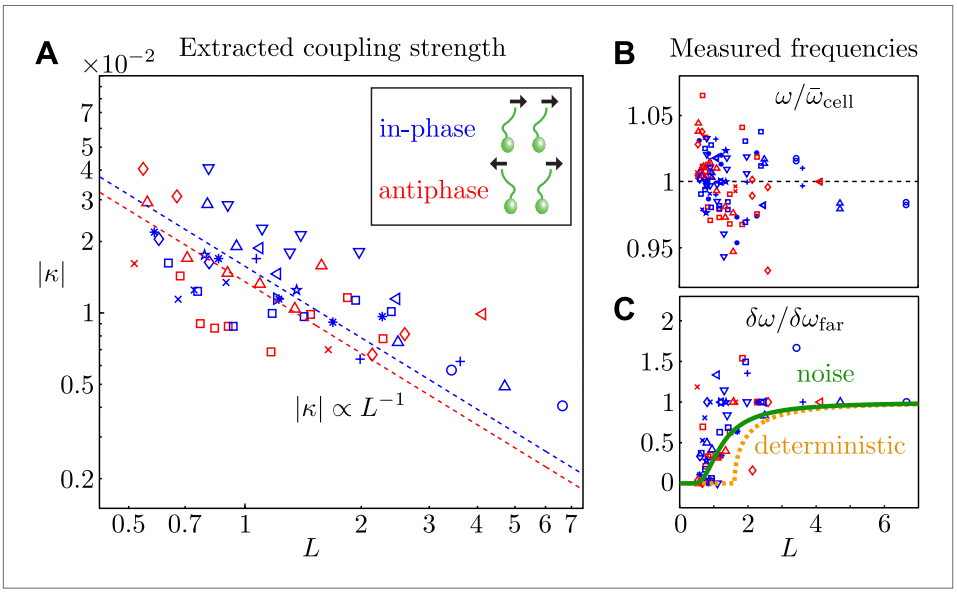

Figure 5. Coupling strength. (**A**) Dimensionless interflagellar coupling strength $\boldsymbol{\kappa} = \boldsymbol{\varepsilon}/\bar{\omega}$ as a function of the scaled spacing $L = d/l$ (log–log scale). The dotted lines represent fits of the form $|\boldsymbol{\kappa}| = k \times L^{-1}$ with $k = 0.016$ (in-phase) and $k = 0.014$ (antiphase). (**B**) Measured beat frequency $\boldsymbol{\omega}/\bar{\omega}_{cell}$ of each flagellum, nondimensionalised by the average value for that cell across several videos. (**C**) Measured frequency difference $\boldsymbol{\delta\omega}/\boldsymbol{\delta\omega}_{far}$ as a function of spacing L. The curves represent the predictions based on the average extracted model parameters in the absence (orange) and presence of noise (green). Symbols represent different pairs of cells, with the in-phase (blue) and antiphase (red) configurations shown.

DOI: 10.7554/eLife.02750.010

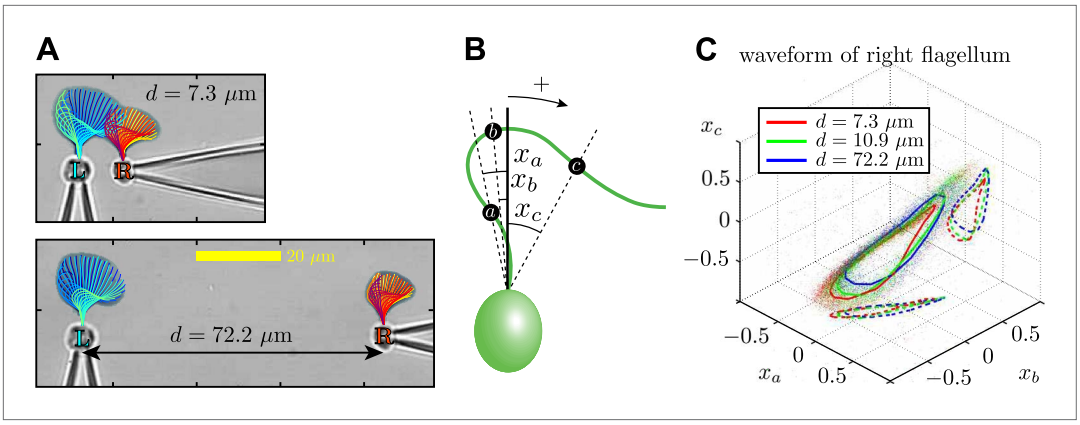

Figure 6. Waveform characteristics. (**A**) Logarithmically-scaled residence time plots of the entire flagella. The displayed waveforms correspond to 1 ms time intervals over several successive flagellar beats. (**B**) Angles x_a, x_b, x_c (in radians) measured and (**C**) their characteristic 3D trajectories. Results are shown for the right flagellum, corresponding to three different interflagellar spacings. As the spacing *d* is increased, the flagellar waveform exhibits a systematic change.

DOI: 10.7554/eLife.02750.011

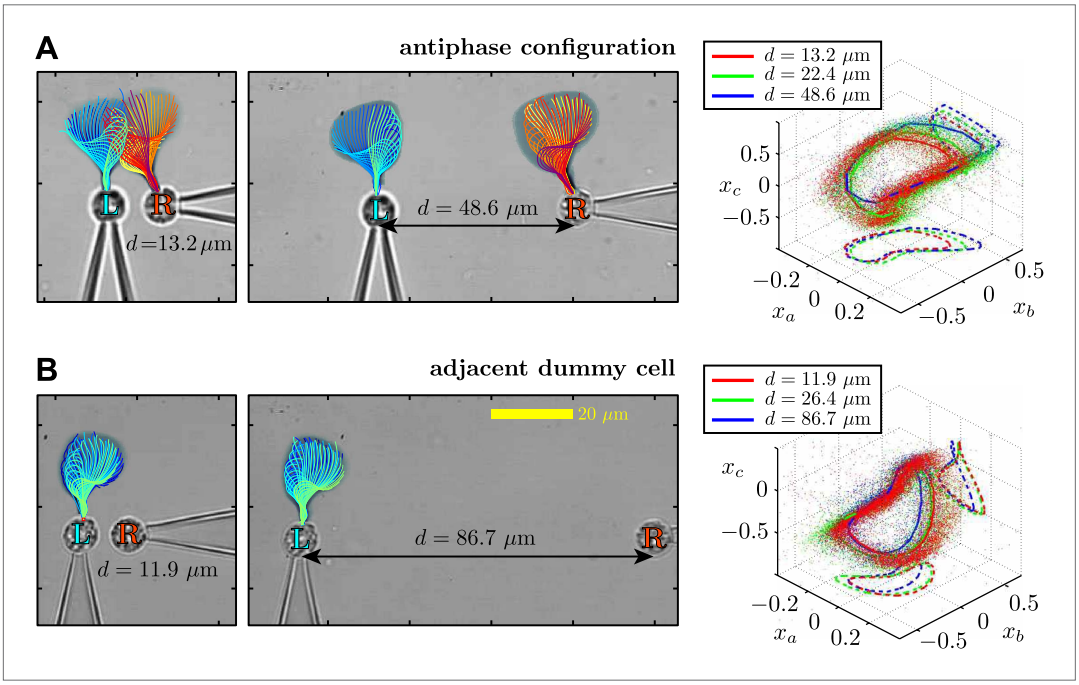

Figure 6—figure supplement 1. Flagellar filaments are tracked for cells in the (A) antiphase state, as well as (B) the situation in which one of the cells does not possess a flagellum (dummy cell).

DOI: 10.7554/eLife.02750.012

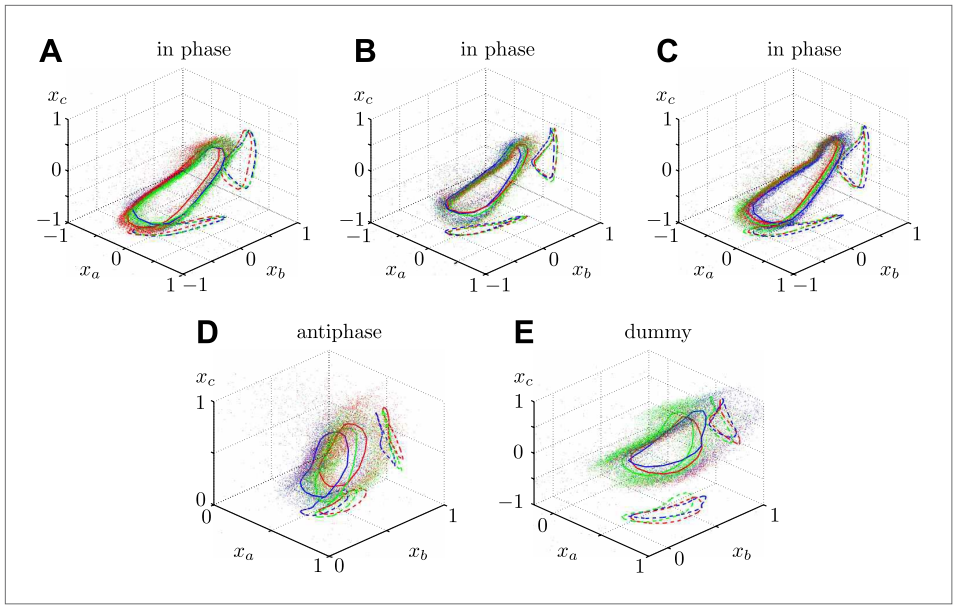

Figure 6—figure supplement 2. Additional waveform data collected for 5 different cells in various geometric configurations.

DOI: 10.7554/eLife.02750.013

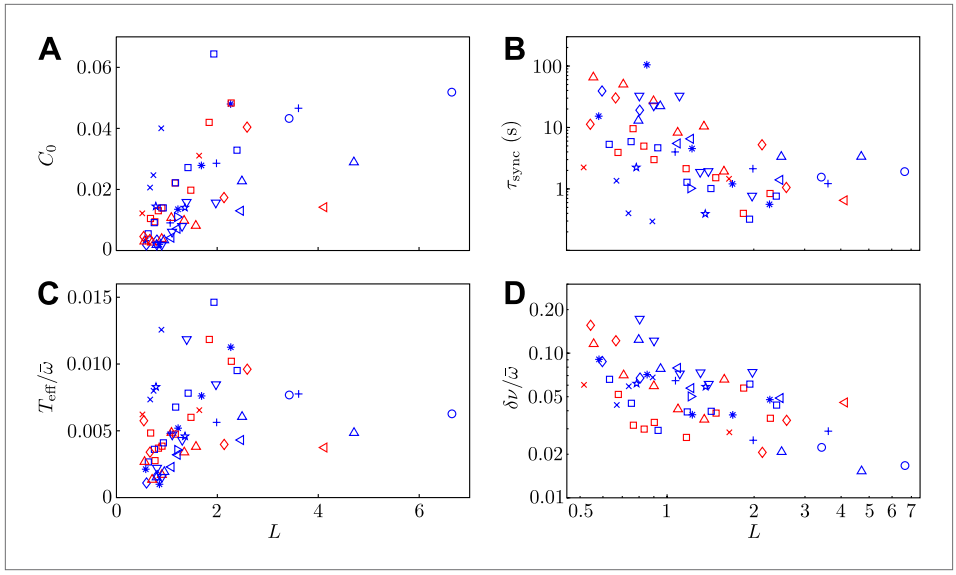

Figure 7. Model parameters. Two of the experimental observables (**A**) C_0 and (**B**) τ_{sync}, and the two additional model parameters (**C**) $T_{\mathrm{eff}}/\bar{\omega}$ and (**D**) $\delta\nu/\bar{\omega}$ are shown as functions of interflagellar spacing for all experiments conducted.

DOI: 10.7554/eLife.02750.015

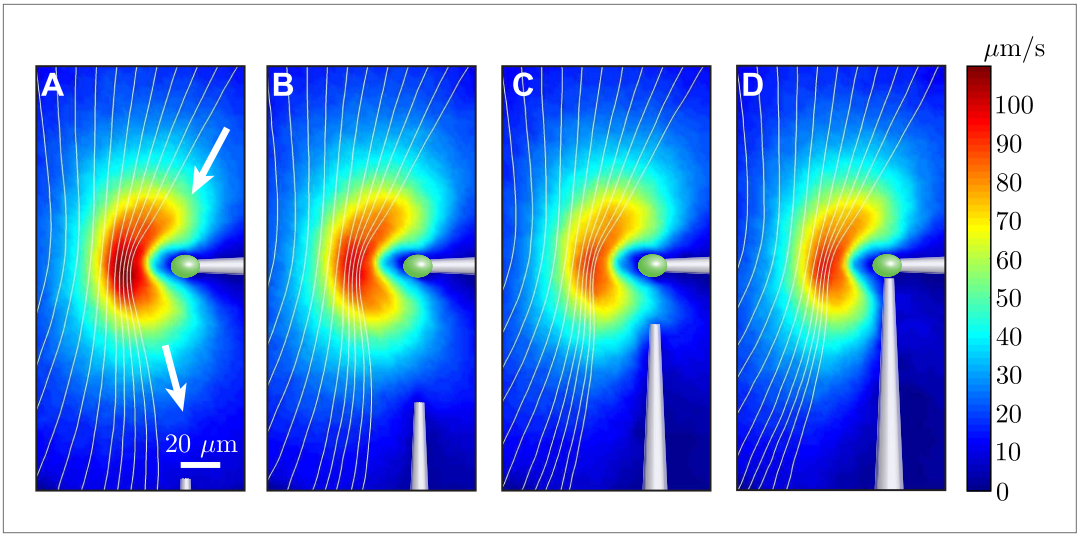

Figure 8. Effect of nearby pipette. The time-averaged flow field associated with one captured cell is measured as a second pipette slowly approaches. This demonstrates that the precise angle from which the cell is held by the micropipette has very little effect on the resultant flow field.

DOI: 10.7554/eLife.02750.016

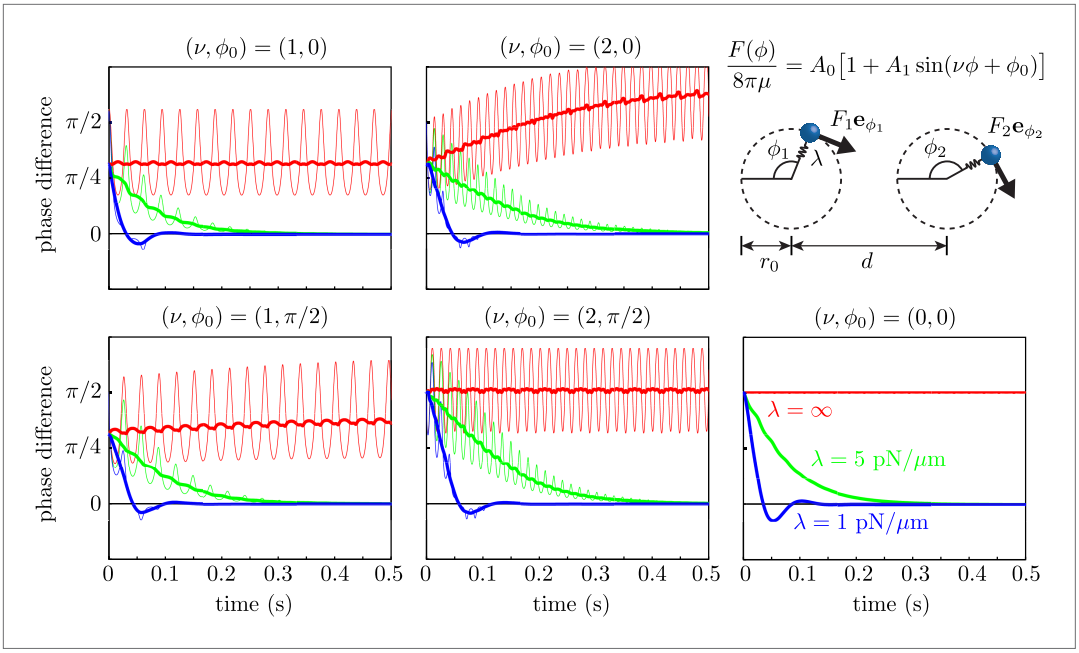

Figure 9. Effect of force modulation. Evolution of the phase difference $\delta = \varphi_1 - \varphi_2$ among two identical model oscillators, each composed of a sphere driven around a circular trajectory by a tangential driving force. The trajectories each possess a radial stiffness λ. Smaller values of λ yield rapid convergence towards synchrony ($\delta = 0$), in a manner essentially independent of the functional form of the driving force. Parameters used are given by $a = 0.75$ μm, $r_0 = 8$ μm, $d = 20$ μm, $A_0 = 1076$ μm²/s and $A_1 = 0.56$.

DOI: 10.7554/eLife.02750.017

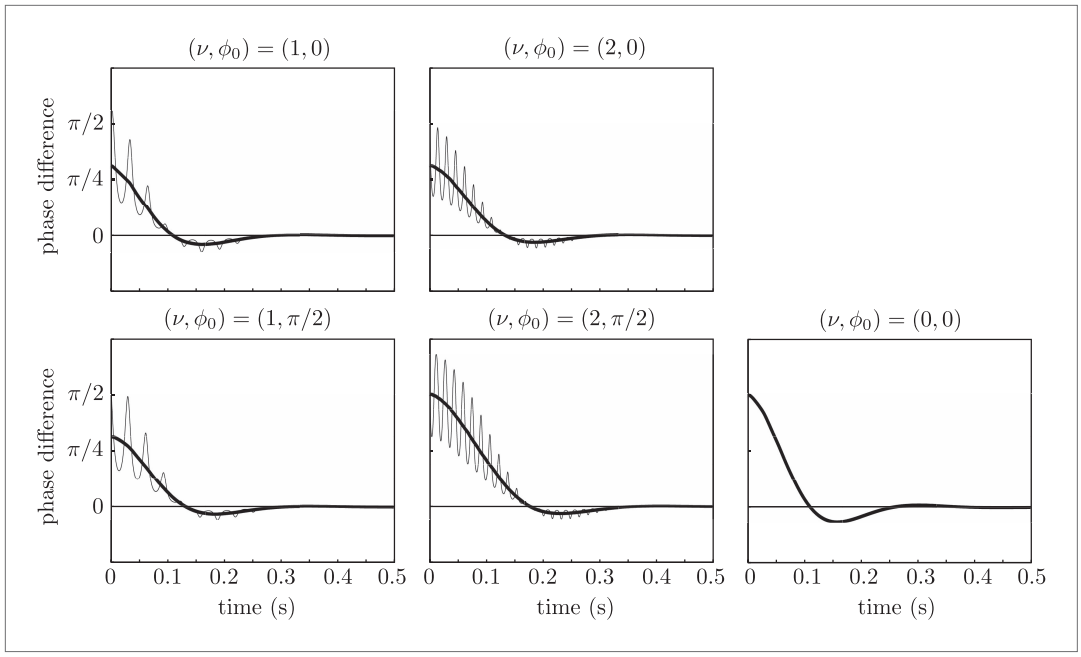

Figure 10. Effect of force modulation. Re-run of the simulations in ***Figure 9*** with properties inspired by real flagella.
DOI: 10.7554/eLife.02750.018